Preprint
UCRL-JC-145544

Characterization of Nanostructural Features in Irradiated Reactor Pressure Vessel Model Alloys

B. D. Wirth, G. R. Odette, P. Asoka-Kumar, R. H. Howell, P. A. Sterne

This article was submitted to
10th International Conference on Environmental Degradation of Materials in Nuclear Power Systems-Water Reactors, Lake Tahoe, NV, August 5-9, 2001

August 1, 2001

U.S. Department of Energy
Lawrence Livermore National Laboratory

This work was performed under the auspices of the United States Department of Energy by the University of California, Lawrence Livermore National Laboratory under contract No. W-7405-Eng-48.

Characterization of Nanostructural Features in Irradiated Reactor Pressure Vessel Model Alloys

Brian D. Wirth
Lawrence Livermore National Laboratory
P.O. Box 808, L-353
Livermore, CA 94550 USA

G. R. Odette
Department of Mechanical Engineering
University of California, Santa Barbara
Santa Barbara, CA 93106 USA

Palakkal Asoka-Kumar
Lawrence Livermore National Laboratory
P.O. Box 808, L-280
Livermore, CA 94550 USA

Richard .H. Howell
Lawrence Livermore National Laboratory
P.O. Box 808, L-280
Livermore, CA 94550 USA

Phil A. Sterne
Lawrence Livermore National Laboratory
P.O. Box 808, L-415
Livermore, CA 94550 USA

Abstract

Irradiation embrittlement in nuclear reactor pressure vessel steels results from the formation of a high number density of nanometer-sized copper rich precipitates and sub-nanometer defect-solute clusters. We present results of small angle neutron scattering (SANS) and positron annihilation spectroscopy (PAS) characterization of the nanostructural features formed in binary and ternary Fe-Cu-Mn alloys irradiated at ~290°C. These complementary techniques provide insight into the composition and character of both types of nanoscale features. The SANS measurements indicate populations of copper-manganese precipitates and smaller vacancy-copper-manganese clusters. The PAS characterization, including both Doppler broadening and positron lifetime measurements, indicates the presence of essentially defect-free Cu precipitates in the Fe-Cu-Mn alloy and vacancy-copper clusters in the Fe-Cu alloy. Thus the SANS and PAS provide a self-consistent picture of nanostructures composed of copper-rich precipitates and vacancy solute cluster complexes and tend to discount high Fe concentrations in the CRPs.

Introduction

The continued safe operation of nuclear reactors and their potential for lifetime extension depends on maintaining the integrity of the reactor pressure vessel (RPV), which embrittles during neutron irradiation. RPV embrittlement results from hardening caused by the formation of a high number density of ultra-fine scale features during irradiation.

Over the last two decades, a combination of theory and experimental techniques has established that nanometer sized copper-manganese-nickel rich precipitates (CRPs), or clusters, are often the dominant embrittling feature in pressure vessel steels[1-19]. A secondary embrittling feature, relatively independent of copper, accumulates with neutron dose and produces significant embrittlement at high fluence, even in low Cu steels[20]. The latter have been termed stable matrix features (SMFs) based on their post-irradiation annealing kinetics[4,13]. Theory and atomistic simulations, as well as the annealing experiments, suggest that the SMFs are three-dimensional, sub-nanometer vacancy-solute (Mn, Cu and Ni) cluster complexes (VSCs) that initially form in displacement cascades[4,6,14]. The balance of CRPs and VSCs depends on the combination of metallurgical and irradiation variables[4,6].

However, there is significant controversy regarding the actual CRP composition[1,5,17,19,26] and up until now, the vacancy character of the SMFs has largely rested on interpretations of annealing signatures and simulation results[4,6,13,14]. The practical implications of such disparities are enormous and impact predictions of embrittlement at higher neutron exposures to be experienced during plant life extension.

Three-dimensional atom probe (3DAP)[17-19,24-27] and small angle neutron scattering (SANS)[8-14,27] have been extensively used to characterize the precipitate nanostructures, including a few cases on the same RPV steels in the same irradiation condition[27]. The 3DAP and SANS results generally reveal similar CRP-type feature number densities, sizes and Mn and Ni contents, which are also consistent with theoretical predictions, but they give somewhat different views of their composition. The 3DAP results have been interpreted to suggest that the nanoscale clusters are copper enriched, but contain significant quantities of iron (> 50%) as well as being microalloyed with manganese, nickel, silicon, and phosphorous[17-19]. In contrast, standard interpretation of a large body of SANS data, including on alloys with systematic variations in the key elements indicate the presence of well-formed CRPs that contain Cu (typically ~70%), Ni and Mn, but little or no Fe[8-14]. There are also alternative candidates for SMFs, including interstitial cluster complexes, dilute atmospheres of solutes and other nanoscale phases associated with a wide variety of elements[4,6,26].

Both SANS and 3DAP have significant limitations. In principle, 3DAP offers the potential of near atomic resolution. However, the resolution is not absolute and is to some extent influenced by trajectory aberrations, including those associated with the complex topology of the evaporation surface at CRPs and SMFs like VSCs[19]. Due to the very small size of these features, positional uncertainties of 0.5 nm or less would artificially place significant numbers of iron atoms in a CRP and solute atoms in the adjoining matrix. The 3DAP technique also suffers from limited statistics associated with sampling very small material volumes [typically on the order of a few million atoms (~1-5x10^{-23} m^3)], can not detect defects or defect clusters and may experience preferential evaporation of solute atoms. While SANS measurements sample much larger material volumes, typically on the order of 10^{-7} m^3, the data analysis relies on non-unique assumptions, particularly regarding the magnetism and composition of CRPs and SMFs, and suffers co-variance and additional non-uniqueness associated with de-convoluting the scattering contributions from multiple, size distributed scattering features.

The objective of this work is to use a combination of positron annihilation spectroscopy (PAS) and SANS to partly mitigate their individual limitations in characterizing the nanostructural features formed in neutron irradiated binary and ternary Fe-Cu-Mn alloys. The SANS technique provides information on the CRP size, number density and volume fractions, as well as providing insight into the precipitate compositions[8-14,27]. Positron annihilation spectroscopy has been used as a defect probe for a wide range of materials[28], including reactor pressure vessel steels[29-33]. The PAS technique is unique in its ability to detect the presence of vacancy and vacancy cluster trapping centers and, most recently, the chemical composition of the trapping site as well[28-39]. Further, positrons are also 'trapped'[a] in Cu precipitates[30-33]. By combining PAS and SANS along with other techniques, including 3DAP, the potential exists to both identify the basic defect character of the SMFs and to resolve the discrepancy between the SANS and 3DAP views of precipitate composition.

Experiment

Materials and Irradiations

A binary Fe-Cu and ternary Fe-Cu-Mn alloy have been examined. The composition, heat treatment history and designations are provided in Table 1. In order to keep the Cu in supersaturated solution prior to irradiation, the alloys were solution annealed at 775°C for 17 hours followed by a 3-minute salt quench to 450°C prior to air-cooling. Coupons of these alloys approximately 1 cm x 1 cm x 2 mm thick were neutron irradiated at ~290°C at two different neutron flux and fluence levels. The irradiation conditions and designations are provided in Table 2.

---

[a] The physical mechanism responsible for positron confinement in CRPs is different than in the case of vacancy defects. Positron localization in CRPs results from the strong positron affinity of copper (-4.81 eV) relative to iron (-3.84 eV)[39], while vacancy trapping is due to missing ionic core(s) resulting in a net attractive potential for a positron with an open volume defect.

SANS

The SANS experiments were performed at the National Institute of Science and Technology (NIST) Center for Neutron Research[40] . Small angle neutron scattering arises from both nuclear (N) and magnetic (M) scattering length density differences between the ferrite matrix and the scattering feature. Thus the samples were measured in a strong magnetic field (~1.7T) that saturated the iron matrix. The scattering from a well-collimated beam of 0.5 nm wavelength neutrons was recorded on a position sensitive detector with a maximum q-range of about 3 nm^{-1}. The scattering data for the radiation induced features were calculated by subtracting background counts, parasitic scattering and normalized scattering from an unirradiated control specimen from the net scattering count recorded in each detector pixel. The corrected data were then converted to absolute scattering cross-sections, $d\Sigma/d\Omega$, by normalizing to a water reference sample, including standard accounting for transmission and sample volumes. The cross section data were then averaged over small increments of q and the angle φ with respect to the magnetic field direction.

The magnetic component of the $d\Sigma/d\Omega(q,\varphi)$ data were analyzed by least-squares fits assuming log-normal size distribution(s) of spherical scattering features. The features were assumed to act as magnetic holes in a saturated ferromagnetic iron matrix. Since the magnetic scattering contrast is precisely known, this assumption provides absolute estimates of the number density and volume fraction of the scattering features. The magnetic to nuclear (M/N) scattering ratio provides information about the composition of the scattering feature(s). In the case of simple binary and ternary Fe-Cu-Mn alloys, the M/N ratio provides a relatively clear indication of precipitate composition. Additional details regarding the SANS experiments and analysis are provided elsewhere[13,14].

PAS

The PAS measurements were performed using the Lawrence Livermore National Laboratory (LLNL) Pelletron facility. The Pelletron is a 3.0 MeV electrostatic accelerator that forms a positron beam with a flux of ~$6.5x10^9$ $e+/m^2$-s from a 70 mCi ^{22}Na source. The use of a high-energy positron beam allows the characterization of bulk specimens, which do not need to be mounted in vacuum and improves the signal to noise ratio by eliminating background radiation from the positron source. The experimental setup and methods to evaluate and de-convolute positron lifetime spectra and measure and interpret Doppler broadened annihilation spectra are described in more detail elsewhere[35,37].

Briefly, thermalized positrons experience a repulsive potential from ionic cores and attractive potential from electrons and open volume defects. Thus vacancy features and regions with strong positron affinity, including nanovoids (VSCs) and CRPs, effectively 'trap' the positrons. Hasegawa and co-workers have shown that nearly all positrons localize and annihilate in a quantum dot type structure of nanoscale pure Cu precipitates formed in a thermally aged Fe-1.0%Cu alloy[32]. Positron annihilation with electrons produces predominately two gamma rays, which are shifted up or down in energy (Doppler shifts) around 0.511 MeV by an amount $\Delta E = 1/2 p_L c$, where p_L is the longitudinal component of the electron-positron momentum in the direction of gamma ray emission[37]. The ΔE can be precisely determined with good signal to noise ratio using a coincidence, two detector setup, which provides the orbital electron momentum spectra (OEMS). Annihilation with more localized 3d transition metal electrons produce Doppler shifts that extend into the high momentum region. In contrast, annihilation with more spatially extended valence electrons in nanovoids makes a negligible contribution to ΔE at high momentum. The exact shape of the ΔE curves depends on the characteristics of the 3d electrons, hence on the atomic species at the annihilation site. Accordingly, analysis of the high momentum region of the Doppler broadened curve can be used to determine the elemental composition in the vicinity of the positron (trapping feature).

Results

This paper reports SANS and PAS results for a binary Fe-0.9% Cu alloy and a ternary Fe-0.9%Cu-1.0%Mn alloy neutron irradiated at about 290°C to neutron fluence (E>1MeV) of 0.8 and $1.0x10^{23}$ n/m^2. SANS measurements have been performed on both alloys at both fluences; however, PAS measurements have only been performed on the alloys at the higher fluence.

SANS

Fe-Cu Alloy. Figure 1 shows the SANS defect scattering cross-section in the neutron irradiated Fe-0.9%Cu (VH) specimen neutron irradiated at 290°C to $0.8x10^{23}$ (Fig. 1a) and $1.0x10^{23}$ n/m^2 (Fig. 1b) as a function of q^2. At the lower fluence, a single feature, log-normal fit to the scattering data (shown by the lines in Figure 1a) resulted in a mean radius, number density and volume fraction of 3.4 nm, about $4x10^{22}$ /m^3 and 0.68%, respectively. The measured R-value of 0.39 (M/N=6.7), is in good agreement with the expected value for a pure copper precipitate (0.37 ± 0.02). For the slightly higher fluence of $1.0x10^{23}$ n/m^2, a two feature, log-normal fit provides excellent agreement with the data, as shown in Figure 1b. The two-feature fit results in estimates of mean radii of 3.4 and 0.9 nm, number densities of $4.6x10^{22}$ /m^3 and $1.2x10^{23}$ /m^3, volume fractions of 0.75 and 0.04% and R-values of 0.39 (M/N=6.7) and 0.82 (M/N=1.5) using a distribution width parameter, β, of 0.4 and 0.2 for feature 1 and 2, respectively.

In both cases, copper precipitates are the dominant scattering feature and the observed R-values are in good agreement with those expected for a pure copper precipitate. At the higher fluence, feature 2 is consistent with small vacancy-solute clusters (VSCs). The R-value of 0.82 and mean size of 0.9 nm corresponds to an atomic volume of approximately 260 lattice sites with a composition of ~60% Cu and 40% vacancies, e.g. 160 Cu atoms and 100 vacancies. The scattering from such features is at least about two times smaller in the K2 irradiation, hence it cannot be reliably detected. This difference bewtween tha P1 and K2 results is not fully understood, but may be partly due to a combination lower fluence and flux and higher temperatures in the latter case.

Fe-Cu-Mn Alloy. Figure 2 shows the SANS defect scattering cross-section in the neutron irradiated Fe-0.9%Cu-1.0%Mn (VD) specimen neutron irradiated at 290°C to $0.8x10^{23}$ (Fig. 2a) and $1.0x10^{23}$ n/m^2 (Fig. 2b) as a function of q^2. At both fluences, a two feature, log-normal fit provides excellent agreement to the scattering data. It is important to note that the precise numerical parameters derived from the two-feature fit are not unique and are somewhat to strongly co-variant, particularly when the sizes of the two features are similar. However, the exact number densities and volume fractions aside, the interpretation that there are multiple scattering features with different R values is very robust and provides important insight on the nanofeatures that form under irradiation.

At the lower fluence of $0.8x10^{23}$ n/m2, the two feature fit resulted in mean radii of 1.8 and 0.5 nm, number densities of $2.5x10^{23}$ and $16.0x10^{23}$ /m3, volume fractions of 0.63% and 0.10%, using a distribution width parameter, β of 0.4 and 0.2 for feature 1 and 2, respectively. The measured R-value of 0.50 (M/N=4) of feature 1 is consistent with a copper precipitate containing about 92% Cu and 8% Mn. The R-value of 0.85 (M/N=1.4) and mean size (0.5 nm) of the second feature corresponds to about 45 atomic volumes, consistent with a population of solute-vacancy clusters (VSCs), containing, for example, about 31 Cu atoms, 8 Mn atoms and 6 vacancies.

At the higher fluence of $1.0x10^{23}$ n/m2, the two feature fit resulted in mean radii of 2.0 and 1.0 nm, number densities of $2.3x10^{23}$ /m^3 and $3.0\ x10^{23}$ /m^3, volume fractions of 0.78 and 0.11% and R-values of 0.47 (M/N=4.6) and 0.71 (M/N=2.0) using a distribution width parameter, β of 0.4 and 0.2 for feature 1 and 2, respectively. In this case, feature 1 are CRPs containing about 94% Cu and 6% Mn and feature 2 is consistent with a population of larger vacancy-solute clusters (VSCs) including Mn, containing for example, about 70% Cu, 18% Mn and 12% vacancies. Notably, the VSCs appear to indicate a decrease in number density and increase in mean size between 0.8 and $1.0x10^{23}$ n/m^2. This is not understood and should be considered in the context of the general issue of non-uniqueness and covariance in multiple feature fits.

PAS

Fe-Cu. In the Fe-Cu alloy neutron irradiated to the higher fluence of about $1x10^{23}$ n/m^2, a substantial increase in the mean positron lifetime from 111 to 232 ps was observed. The positron lifetime fitting procedure yielded three distinct components, with lifetime and intensities of 91 ps/37%, 222 ps/43% and 516 ps/20%. The first lifetime component can be interpreted as positron annihilation before trapping, while the two longer lifetime components are interpreted as positron trapping in vacancy-type defects. Calculations indicate that a positron lifetime of about 220 ps corresponds to a small vacancy cluster containing 3-5 vacancies, while a lifetime of 520 ps corresponds to a 3-dimensional vacancy cluster containing 50 or more vacancies and a radius of 0.5 nm or larger. Similar long lifetime values would be expected for positron annihilation in surface states in metals, but this can be ruled out here due to the highly penetrating 3 MeV positron beam, and the absence of any such surface signal in the unirradiated control

samples. The larger vacancy clusters are consistent with the secondary feature observed in the SANS measurements. To the best of our knowledge, this represents the first positron lifetime measurement of such a significant population of long-lifetime component (large vacancy clusters) in Fe-based steels or alloys irradiated at 288°C.

The normalized OEM spectrum is shown in Figure 3a, along with the comparably normalized spectrum for well-annealed elemental copper. In contrast to observations of thermally aged Fe-Cu (VH) specimens, performed by both Hasegawa and co-workers[32] and our group[41,42], the OEM spectrum is not identical to elemental copper. In this case, the OEM spectrum shows a peak at low momentum [p_L < 1 atomic unit (a.u.)] values and shows a slight peak, indicative of copper at higher (p_L >~2.5 a.u.) values. Consistent with the positron lifetime measurements, these coupled observations suggest significant positron trapping at vacancy-Cu cluster complexes (VSCs). Additionally, the peak at higher momentum values, as well as the indication of positron annihilation prior to trapping, suggest that some positron annihilation also occurs in the copper precipitates.

Fe-Cu-Mn Alloy. In contrast to the Fe-Cu alloy, the neutron irradiated Fe-Cu-Mn alloy (irradiated to a fluence of about $1x10^{23}$ n/m^2) showed only a slight increase in mean positron lifetime from 110 to 120 ps. The positron lifetime fitting procedure yielded two distinct components for the Fe-Cu-Mn alloy, with lifetime and intensity values of 87 ps/31% and 134 ps/69%, respectively. The positron trapping model was entirely successful in fitting the data and, the short (relative to the bulk value of ~110 ps) value of the first lifetime indicates positrons annihilation prior to trapping. Notably, the second lifetime of 134 ps is much shorter than the 170 ps value experimentally measured for a free vacancy[34]. At this time, it is not clear whether this result implies that a reduced vacancy concentration or that the vacancies are bound to Cu-Mn complexes.

The OEM spectrum, normalized to the solution annealed VD control is shown in Figure 3b, along with the comparably normalized spectrum for well-annealed elemental copper. As we have previously shown for thermally aged Fe-Cu-Mn specimen[41,42], the OEM spectrum is close to that for pure copper. The small difference is consistent with the presence of a modest fraction of either Mn or Fe in the precipitates. Note Mn enrichment is consistent with both thermodynamic predictions of Mn segregation to the precipitates and the SANS magnetic to nuclear scattering ratio results. Overall, however, the momentum spectrum in the Fe-Cu-Mn alloy indicates that the CRPs are highly enriched in Cu.

Discussion

The results from the complementary SANS and PAS characterization of nanoscale features in neutron irradiated Fe-Cu-Mn alloys are consistent with the identification of copper rich precipitates (CRPs) and stable matrix features (SMFs) as the nanoscale features responsible for embrittlement. The SANS measurements are consistent with rapid precipitate nucleation followed by a slow coarsening mediated growth with increasing fluence. Increased precipitate volume fractions are observed in both the Fe-Cu and Fe-Cu-Mn alloys with increasing fluence along with small increases in the mean size and little change in precipitate number density (slight increase in Fe-Cu, slightly larger decrease in Fe-Cu-Mn). Notably, the VSCs in the Fe-Cu-Mn alloy showed a dramatic decrease in number density and increase in mean size between 0.8 and $1.0x10^{23}$ n/m^2.

The two-detector, coincidence orbital electron momentum (OEM) PAS results on the higher fluence Fe-Cu-Mn alloy is nearly identical to pure copper, in agreement with the SANS results which suggest that the precipitates are approximately 94% Cu and 6% Mn. However, the OEM spectrum of the higher fluence Fe-Cu alloy does not resemble elemental Cu. The SANS measurements of the Fe-Cu alloy did indicate the presence of two scattering features, larger CRPs and smaller SMFs. The R-value (magnetic to nuclear scattering ratio) of the CRPs is consistent with pure copper precipitates, but the precipitates are much larger with a substantially smaller number density than those observed in the Fe-Cu-Mn alloys. In addition, the positron lifetime measurements revealed a substantial long lifetime component (222 ps/43% and 516 ps/20%) in the high fluence Fe-Cu alloy. This is consistent with a population of large (> 50 vacancies) vacancy clusters. The OEM spectra confirm the presence of vacancy clusters and indicate an association with copper. Thus, we believe that this result is indicative of the competition between the copper precipitates and the vacancy clusters as positron trapping (confinement) sites. Future low temperature post-irradiation annealing of this and other neutron irradiated Fe-Cu specimens (to dissolve the vacancy clusters but not significantly alter the precipitates) should confirm this hypothesis.

Notably, these very same alloys have been examined with three-dimensional atom probe (3DAP) at the higher fluence condition (P1)[27,43]. Indeed, atom probe wires were cut from the same samples, which we have characterized with SANS and PAS[41,42]. The 3DAP results are reasonably consistent in observing small (~ 1 nm) and large (~ 2.5 nm) copper clusters in the Fe-0.9% Cu alloy and a much higher number density of smaller, ~1.8 nm copper precipitates in the Fe-0.9% Cu-1.0% Mn alloy[43]. However, the estimated 3DAP precipitate compositions are inconsistent with these SANS and PAS results. Miller estimated compositions of ~73% Cu and 27% Fe for the large precipitates in the Fe-Cu alloy and 44% Cu, 4% Mn and 52% Fe in the Fe-Cu-Mn alloy[43].

While the SANS and PAS results can not discount some (~10%) Fe within the precipitates, it is difficult to rationalize these results with compositions of 27-52% Fe. For example, in the high fluence Fe-0.9% Cu alloy, a precipitate composition of 73% Cu and 27% Fe would result in a magnetic to nuclear scattering ratio of about 13.5 (R=0.27), considerably higher than the measured value of 6.7. Additionally, using this precipitate composition to calculate the nuclear scattering contrast (and thereby neglect any assumptions of precipitate magnetization) requires a precipitate volume fraction of 1.5%, which requires more Cu (1.5%x0.73~1.1%) than is available in the Fe-0.9% Cu alloy. Similarly, using the 3DAP estimated precipitate composition of 44% Cu, 4% Mn and 52% Fe in the high fluence Fe-0.9% Cu-1.0% Mn alloy produces a magnetic to nuclear scattering ratio of 8.2 (R=0.35), considerably higher than the measured value of 4.6. And, a volume fraction of 1.76% is required to match the measured nuclear scattering cross-sections, resulting in precipitate number densities that are higher than those observed by 3DAP.

It is also useful to compare the results in this study of the Fe-Cu and Fe-Cu-Mn alloy in the K2 irradiation condition (Figure 1a and 2a) to estimates of Cu and Mn precipitation based on combined electrical resistivity and Seebeck coefficient (CRSC) measurements[44]. For the Fe-Cu alloy, the total Cu precipitation from SANS is estimated to be 0.68%, compared to 0.70±0.05 from the CRSC measurements. For the Fe-Cu-Mn alloy, the total Cu plus Mn, estimated in both the precipitate and secondary feature, is ~ 0.71% compared to 0.71% from the CRSC evaluation. The SANS results suggest that the fraction of Mn in the precipitates is about 8% compared to an estimate of about 17% from the CRSC data. While differences between the SANS and CRSC results are within overall uncertainties arising from a variety of sources, a small amount of Fe in the precipitates could reconcile the differences. However, the CRSC, SANS and PAS results are all inconsistent with the much larger amounts of Fe that are indicated by the interpretation of 3DAP results noted above.

Conclusions

A complementary small angle neutron scattering (SANS) and positron annihilation spectroscopy (PAS) characterization of neutron irradiated binary and ternary Fe-Cu-Mn alloys is presented. The results provide insight into the character and composition of the nanostructural features responsible for irradiation embrittlement of nuclear reactor pressure vessel steels. The SANS results clearly indicate the presence of two scattering features. The dominant features are copper rich precipitates, which coarsen slightly with increasing fluence, while the secondary feature is consistent with vacancy-solute cluster complexes. The PAS results clearly reveal the presence of large (> 20) vacancy clusters and indicate an association with copper in the Fe-Cu alloy and the presence of nearly pure copper precipitates in the Fe-Cu-Mn alloy. While the change in dominant positron trap between the Fe-Cu and Fe-Cu-Mn alloys is not understood at this time, the PAS results are consistent with the SANS results and the identification of vacancy-solute cluster complexes as the stable matrix features (SMFs). Further, the results of this work tend discount a large concentration of Fe (> about 20%) in the precipitates. Future work will focus on performing PAS measurements on the lower fluence Fe-Cu-Mn alloys and clarifying these issues.

Acknowledgements

This work was performed under the auspices of the U.S. Department of Energy by the University of California, Lawrence Livermore National Laboratory under contract No. W-7405-Eng-48 with partial support provided from Basic Energy Research, Division of Materials Science and from the US Nuclear Regulatory Commission under contract number NRC-04-94-049. We would like to acknowledge the contributions of Doug Klingensmith and Matt Alinger (UCSB) and Drs. J. Barker and C. Glinka (NIST) as well as the support of the National Institute of Standards and Technology, U.S. Department of Commerce, in providing the neutron research facilities used in this work.

References

1. G. R. Odette, *Scripta Met.* **11**, (1983) 1183.
2. G. R. Odette and G. E. Lucas, *Proceedings of the Second International Symposium on Environmental Degradation of Materials in Nuclear Reactors - Water Reactors*, J. T. A. Roberts, J. R. Weeks, and G. J. Theus, eds., American Nuclear Society, LaGrange Park, IL (1986) 345.
3. S. B. Fisher and J. T. Buswell, *Int. J. of Pressure Vessels and Piping* **27** (1987) 91.
4. G. R. Odette, *MRS Soc. Symp. Proc.* **373** (1995) 137.
5. G. R. Odette, C. L. Liu and B. D. Wirth, *MRS Symp. Proc.* **439** (1997) 457.
6. G. R. Odette and B. D. Wirth, *J. Nucl. Mater.* **251** (1997) 157.
7. G. R. Odette, *Neutron Irradiation Effects in Reactor Pressure Vessel Steels and Weldments*, IAEA IWG-LMNPP-**98/3**, International Atomic Energy Agency, Vienna (1998) 438.
8. G. R. Odette and G. E. Lucas, *Radiation Effects & Defects in Solids* **144** (1998) 189.
9. F. Frisius, R. Kampmann, P. A. Beaven, and R. Wagner, in Dimensional Stability and Mechanical Behavior of Irradiated Metals and Alloys-VI, BNES, London 1983, 171.
10. P. A. Beaven, F. Frisius, R. Kampmann, and R. Wagner, in Proc. Second Int'l Symp. on Environmental Degradation of Materials in Nuclear Reactors, Eds., J. T. A. Roberts, J. R. Weeks and G. J. Theus, American Nuclear Society, LaGrange Park, IL (1986) 400.
11. P. A. Beaven, F. Frisius, R. Kampmann, R. Wagner, and J. R. Hawthorne, ASTM-STP1011, American Society for Testing and Materials, Philadelphia, PA (1989) 243.
12. J. A. Fint, Masters Thesis, University of California, Santa Barbara, 1990.
13. E. V. Mader, *Kinetics of Irradiation Embrittlement and the Post-Irradiation Annealing of Nuclear Reactor Pressure Vessel Steels*, Ph.D. Dissertation, University of California Santa Barbara (1995).
14. B. D. Wirth, *On the Character of Nano-scale Features in Reactor Pressure Vessel Steels Under Neutron Irradiation*, Ph.D. Dissertation, University of California, Santa Barbara (1998).
15. W. J. Phythian and C. A. English, *J. Nuc. Mat.* **205** (1993) 162.
16. T. J. Williams and W. J. Phythian, ASTM-STP1270, American Society for Testing and Materials, Philadelphia, PA (1996), 191.
17. P. Pareige and M. K. Miller, *App. Surf. Sci.* **94/95** (1996) 370.
18. P. Pareige, K. F. Russell, and M. K. Miller, *App. Surf. Sci.* **94/95** (1996) 362.
19. P. Pareige, PhD Thesis, Rouen University (1994).
20. E. D. Eason, J. E. Wright, and G. R. Odette, *Improved Embrittlement Correlations for Reactor Pressure Vessel Steels*, NUREG/CR-6551, (1998).
21. E. D. Eason, J. E. Wright, E. E. Nelson, G. R. Odette, and E. V. Mader, *Nuc. Eng. & Des.* **179** (1998) 257.
22. E. D. Eason, J. E. Wright, G. R. Odette, and E. Mader, *Models for Embrittlement Recovery Due to Annealing of Reactor Pressure Vessel Steels*, NUREG/CR-6327, 1995.
23. G. R. Odette, E. V. Mader, G. E. Lucas, W. J. Phythian, and C. A. English, ASTM-STP1175, American Society for Testing and Materials, Philadelphia, PA (1993) 373.
24. M. K. Miller and M. G. Burke, *J. Nuc. Mat.* **195** (1992) 68.
25. M. K. Miller and M. G. Burke. ASTM-STP-1046 Volume II, American Society for Testing and Materials, Philadelphia, PA (1990) 107.
26. M. K. Miller, P. Pareige and M. G. Burke, Materials Characterization, **44** (2000) 235.
27. B. D. Wirth, G. R. Odette and M. K. Miller, to be published.
28. P. Hautojarvi and C. Corbel in Positron Spectroscopy of Solids, ed. Dupasquier and Mills (IOS Press Amsterdam, 1995) p. 491.
29. G. Brauer, L. Liszkay, B. Molnar and R. Krause, *Nuclear Engineering and Design* **127** (1991) 47.
30. W.J. Phythian. N. DeDiego, J.Mace and R.J. McElroy, in Effects of Radiation on Materials: 16th Int. Symp. ASTM STP 1175, eds. A.S. Kumar, D.S. Gelles, R.K. Nanstad and E.A. Little (American Society for Testing and Materials, Philadelphia, 1994) 462.
31. G. Brauer, M.J. Puska, M. Sob and T. Korhonen, *Nuclear Engineering and Design* **158** (1995) 149.
32. Y. Nagai, M Hasegawa, Z. Tang, A. Hempel, K. Yubata, T. Shimamura, Y. Kawazoe, A. Kawai and F. Kano, *Phys. Rev. B* **61** (2000) 6574.
33. Y. Nagai, Z. Tang, M. Hassegawa, T. Kanai and M. Saneyasu, *Phys. Rev. B* **63** (2001) 134110.
34. P. Hautojarvi, T. Judin, A. Vehanen, J. Yli-Kauppila, J. Johansson, J. Verdone and P. Moser, *Solid State Comm.* **29** (1979) 855.
35. R.H. Howell, P.A. Sterne, J. Hartley, T.E. Cowan, Appl. Surf. Sci. **149** (1999) 103.

36. J.H. Hartley, R.H. Howell, and P.A. Sterne, *Application of Accelerators in Research and Industry*, eds. D.L. Duggan and I.C. Morgan, American Institute of Physics, New York (1999).
37. P. Asoka-Kumar, M. Alatalo, V. J. Ghosh, A. C. Kruseman, B. Nielsen and K. G. Lynn, *Phys. Rev. Letters* **77** (1996) 2097.
38. P. Asoka-Kumar, *Materials Science Forum* **255-257** (1997) 166.
39. M.J. Puska, P. Lanki and R. M. Niemen, *J. Phys. Condens. Matter* **1** (1989) 6081.
40. C. J. Glinka, J. M. Rowe and J. G. laRock, *J. of Applied Crystallography* **19** (1986) 427.
41. B. D. Wirth, P. Asoka-Kumar, R. H. Howell, G. R. Odette, and P. A. Sterne, MRS Soc. Symp. Proc **650** (2001)R6.5.
42. B. D. Wirth, P. Asoka-Kumar, R. H. Howell, G. R. Odette, and P. A. Sterne, "Positron Annihilation Spectroscopy and Small Angle Neutron Scattering Characterization of Nanostructural Features in Neutron Irradiated Fe-Cu-Mn Alloys", submitted to *Phys. Rev. B* (2001).
43. M. K. Miller, B. D. Wirth and G. R. Odette, "Precipitation in Neutron Irradiated Fe-Cu and Fe-Cu-Mn Model Alloys: A Comparison of APT and SANS Data", in preparation for submission to *App. Surf. Sci* (2001).
44. G. R. Odette, C. Cowan and D. Gragg, "Use of Combined Electrical Resistivity and Seebeck Coefficient Measurements to Characterize Solute Redistribution Under Irradiation and Thermal Aging", this conference proceedings.

Table 1. Nominal composition and heat treatments of the alloys used in the SANS characterization.

Alloy	Description	Cu (wt %)	Mn (wt %)	Heat treatment
VB	Fe-Mn binary	.0	1	1
VD	Fe-Cu-Mn ternary	.9	1	1
VH	Fe-Cu binary	.9	0	1

+ Heat treatment

1. Solution annealed at 775 °C for 17 hours, 450 °C salt quench for 3 minutes, air cool.

Table 2. Neutron irradiation conditions used in this study.

Condition Code	T_i (°C)	neutron flux (10^{16} n/m^2-s)	neutron fluence (10^{23} n/m^2)
K2	290	.5	.8
P1	288	.7	1.0

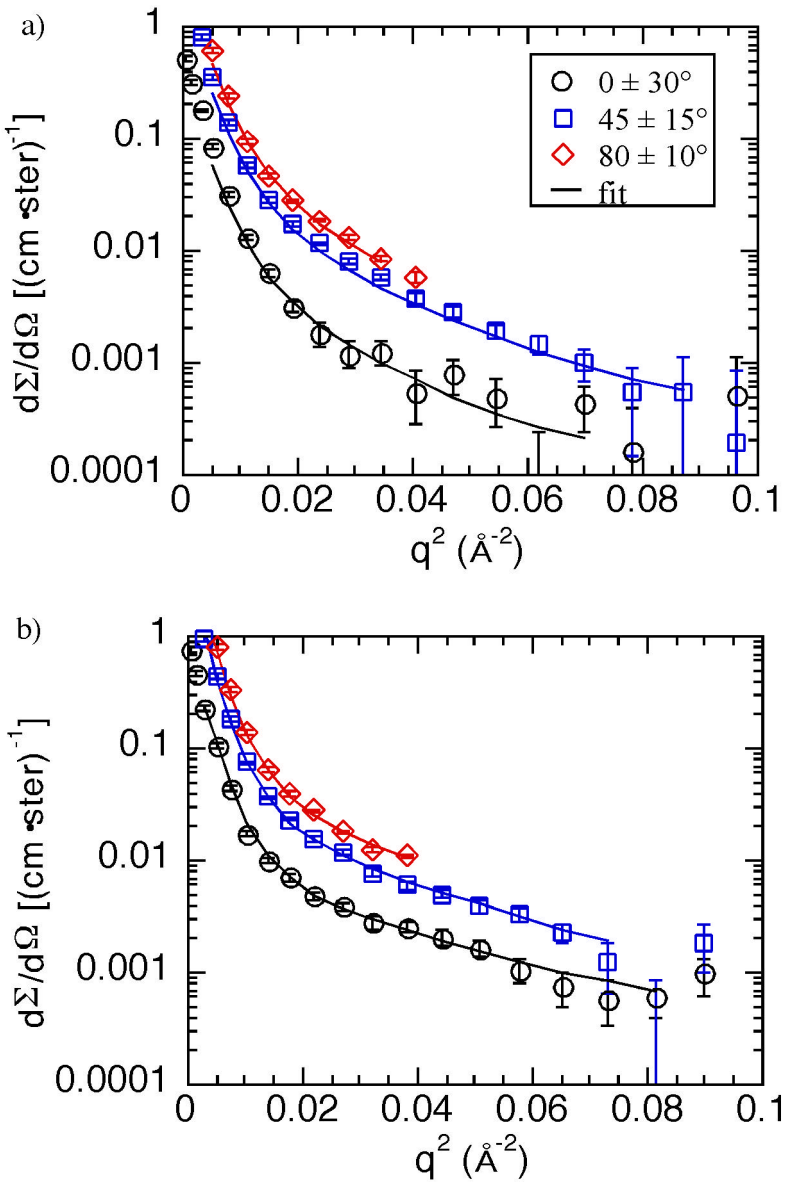

Figure 1 -- Small angle neutron scattering defect cross-sections (symbols) and fit results (lines) at 0±30° (circles), 45±15° (squares) and 80±10° (diamonds) for the Fe-0.9% Cu alloy, neutron irradiated at about 290°C to a) 0.8×10^{23} and b) 1.0×10^{23} n/m2.

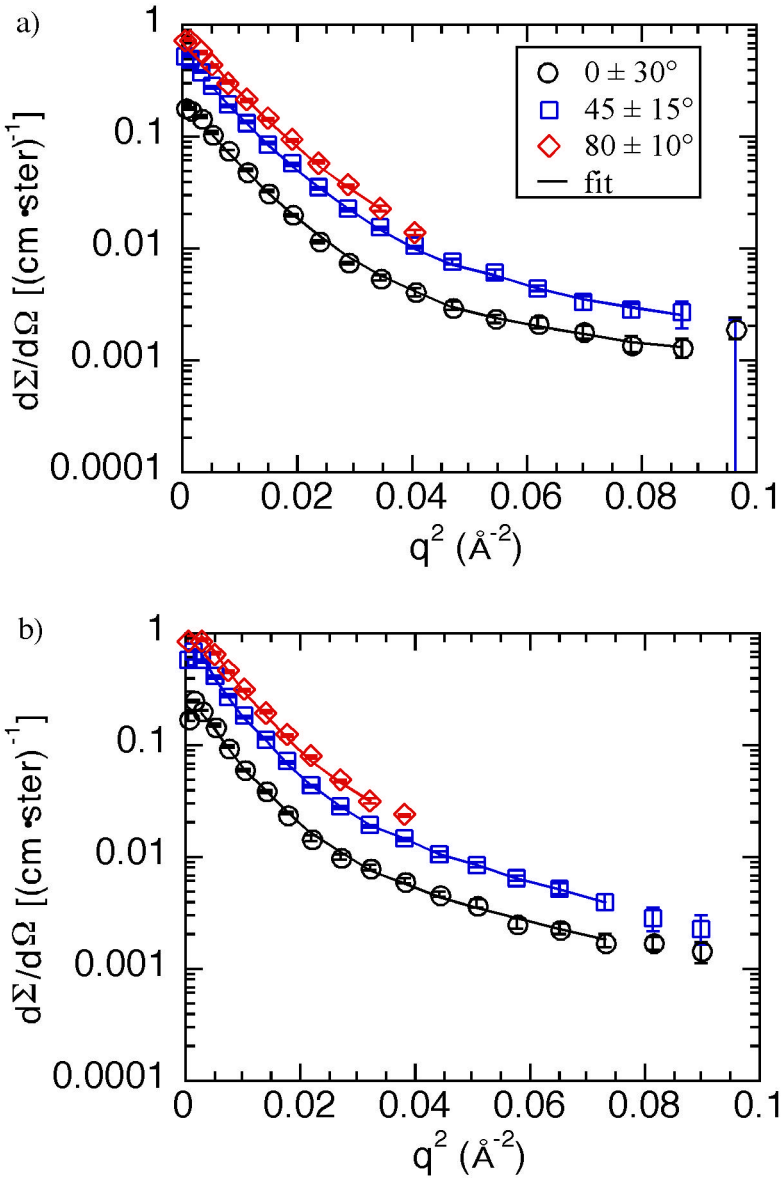

Figure 2 -- Small angle neutron scattering defect cross-sections (symbols) and fit results (lines) at 0±30° (circles), 45±15° (squares) and 80±10° (diamonds) for the Fe-0.9% Cu-1.0% Mn alloy, neutron irradiated at about 290°C to a) 0.8×10^{23} and b) 1.0×10^{23} n/m^2.

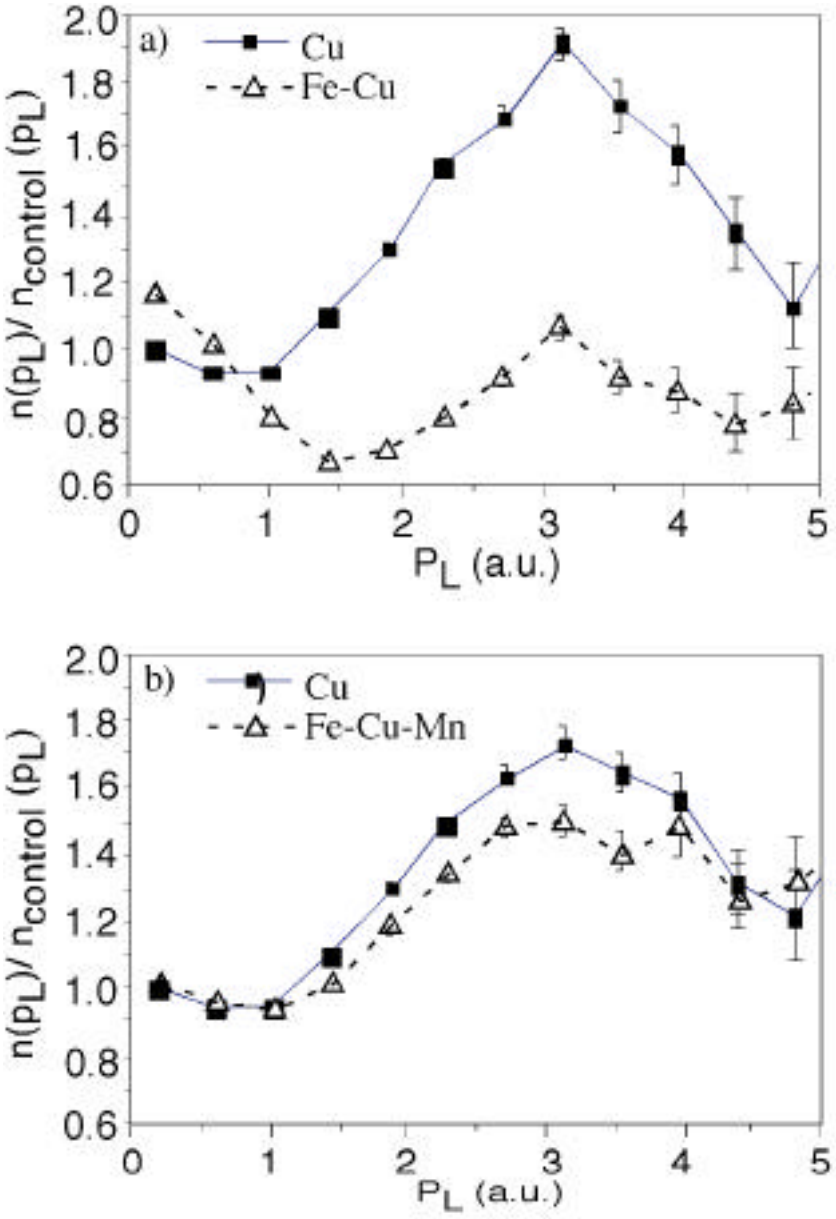

Figure 3 -- Orbital electron momentum spectra of positron annihilation photons for the a) Fe-Cu (VH) and b) Fe-Cu-Mn (VD) alloys neutron irradiated at 288°C to a fluence of 1.0×10^{23} n/m^2 (P1). The spectra have been normalized to the corresponding un-irradiated control specimen and the correspondingly normalized curves of elemental Cu are shown for comparison.